Supplement of Clim. Past, 22, 825–843, 2026
https://doi.org/10.5194/cp-22-825-2026-supplement

Climate of the Past
Open Access
EGU

Supplement of

Growth and decay of the Iceland Ice Sheet through the last glacial cycle

Alexis Arturo Goffin et al.

Correspondence to: Alexis Arturo Goffin (aagoffin@mun.ca)

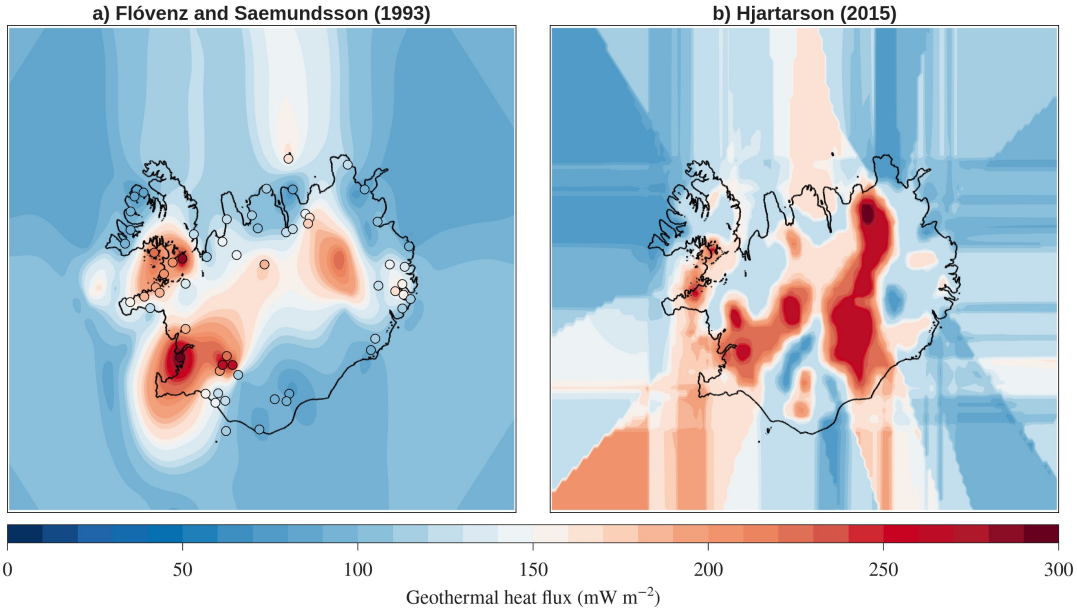

Figure S1. Geothermal heat flux (GHF) fields used as model boundary conditions. (a) GHF field interpolated from borehole measurements (filled circles) compiled by Flóvenz and Saemundsson (1993), and (b) GHF field from Hjartarson (2015).

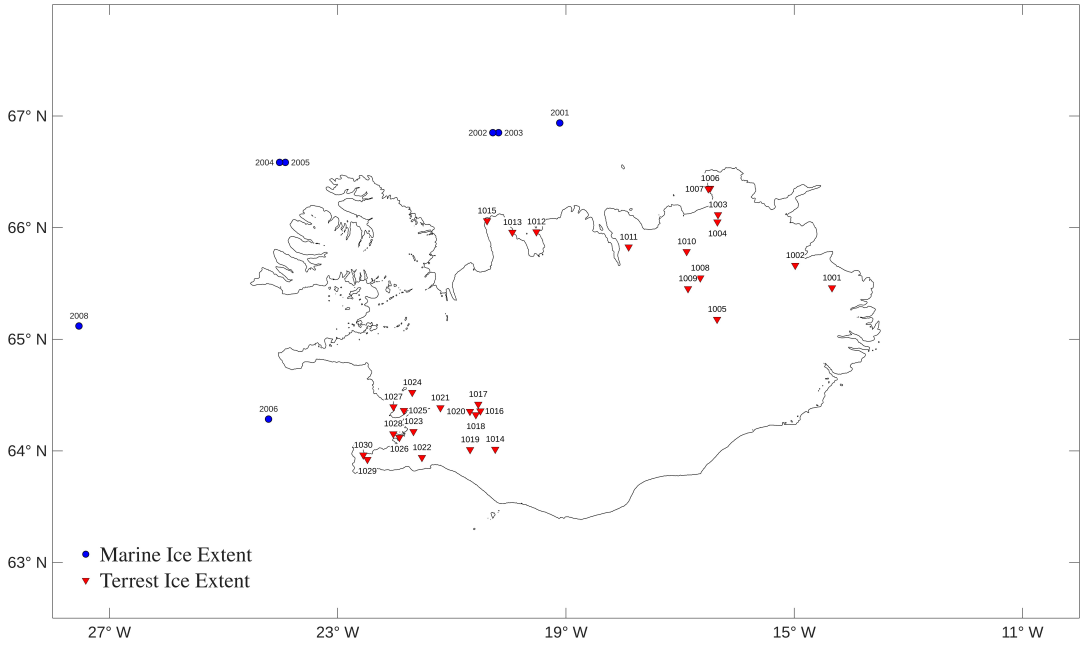

Figure S2. Iceland observational constraint database with site locations and identification numbers for past ice thickness data (paleoH), and past ice extent data (paleoExt).

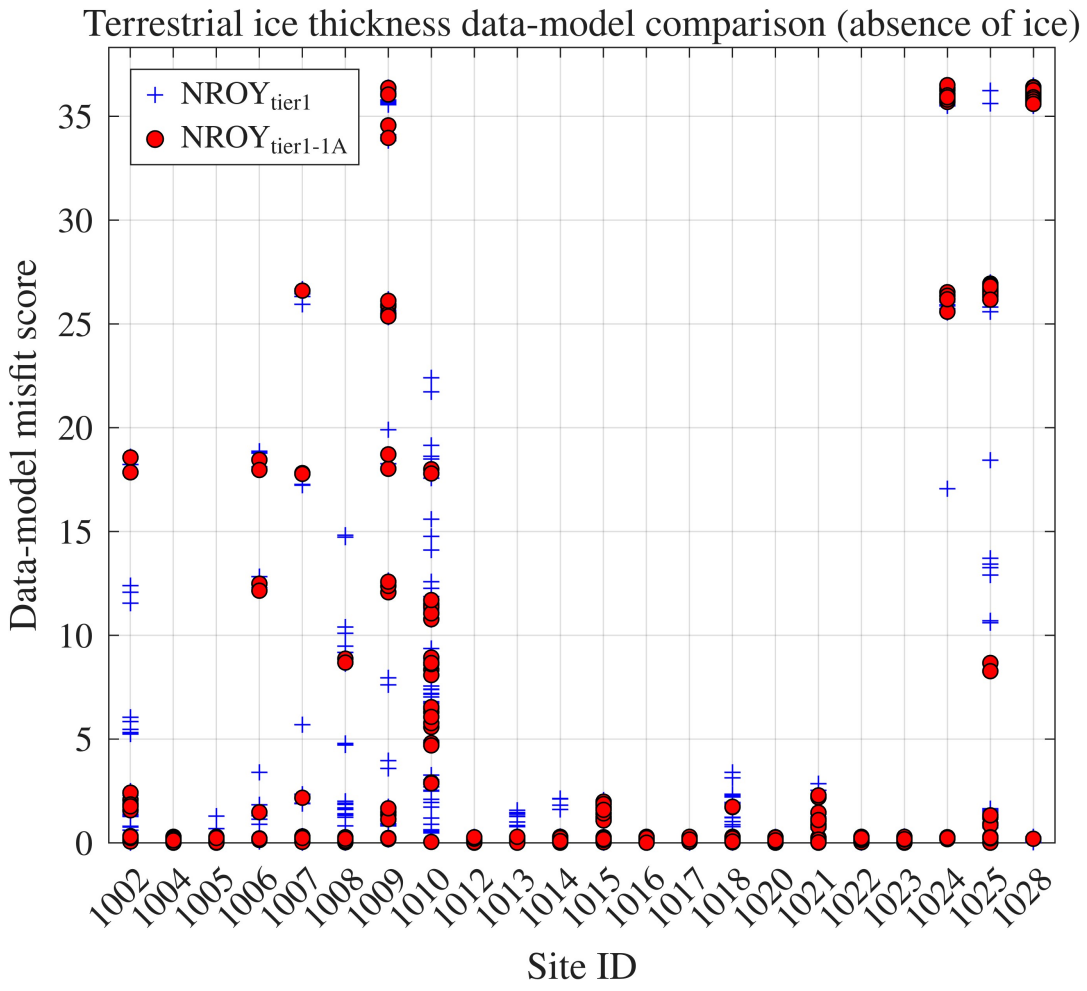

Figure S3. Past ice thickness misfit scores (absence of ice). The data ID locations are shown in Fig. S2.

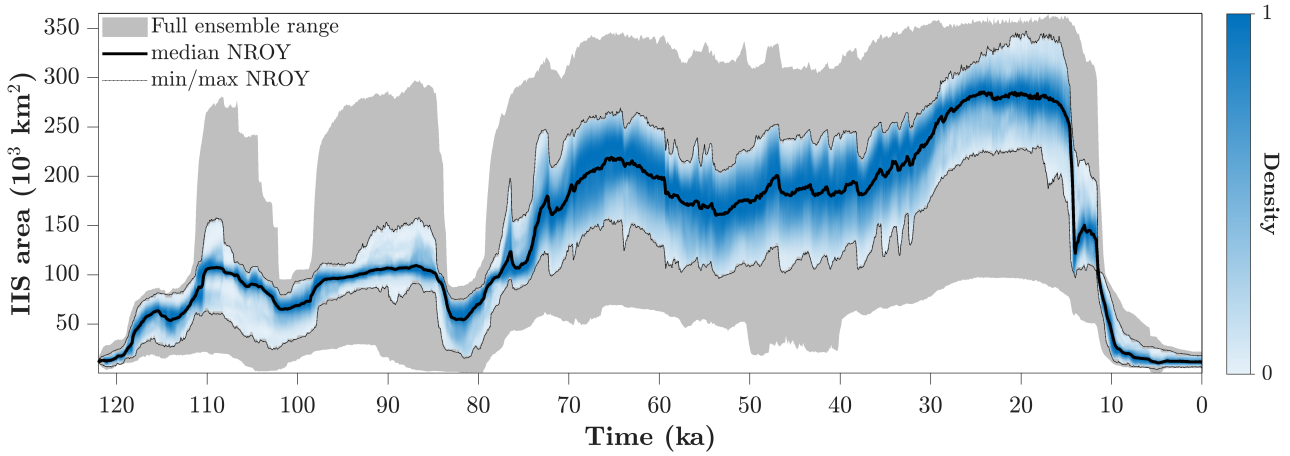

Figure S4. Time series of IIS area during the last glacial cycle. Initial full ensemble (gray shaded area) and sieved not-ruled-out-yet ($NROY_{tier1}$) sub-ensemble (blue distribution) with median $NROY_{tier1}$ (black curve).

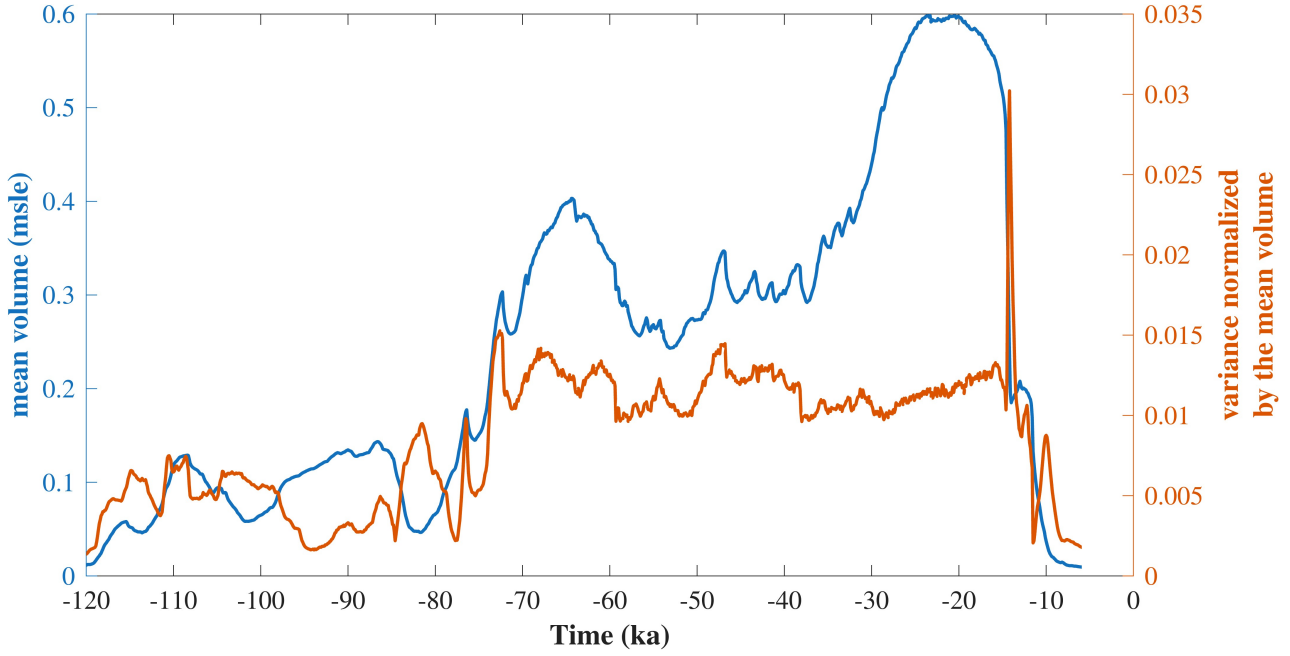

Figure S5. Time series of IIS mean volume (left axis) and variance normalized by the mean volume (right axis) during the last glacial cycle for the $NROY_{tier1}$ subset.

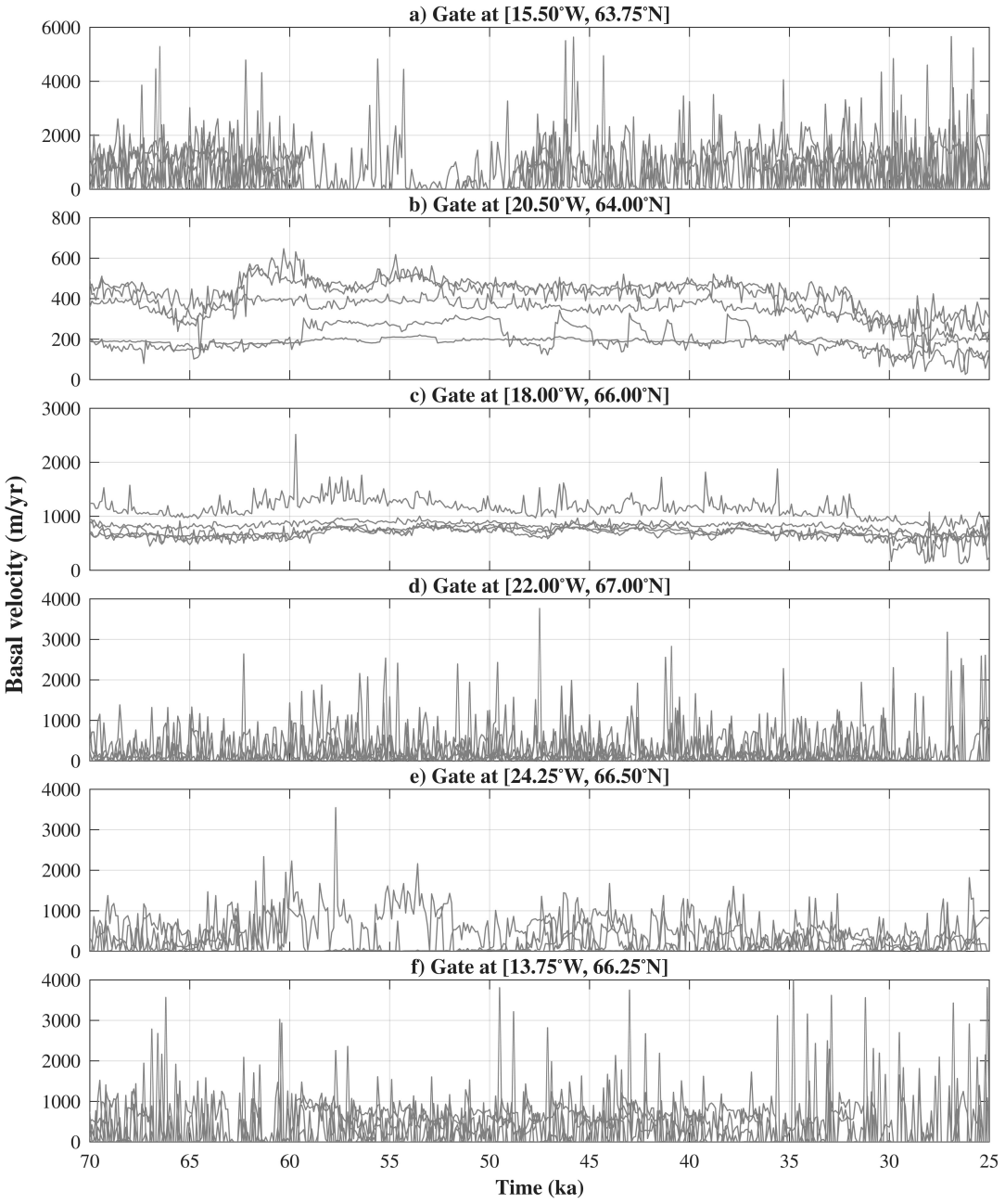

Figure S6. Basal velocity at six ice stream gates of the IIS for 5 $\text{NROY}_{\text{tier1}}$ runs.

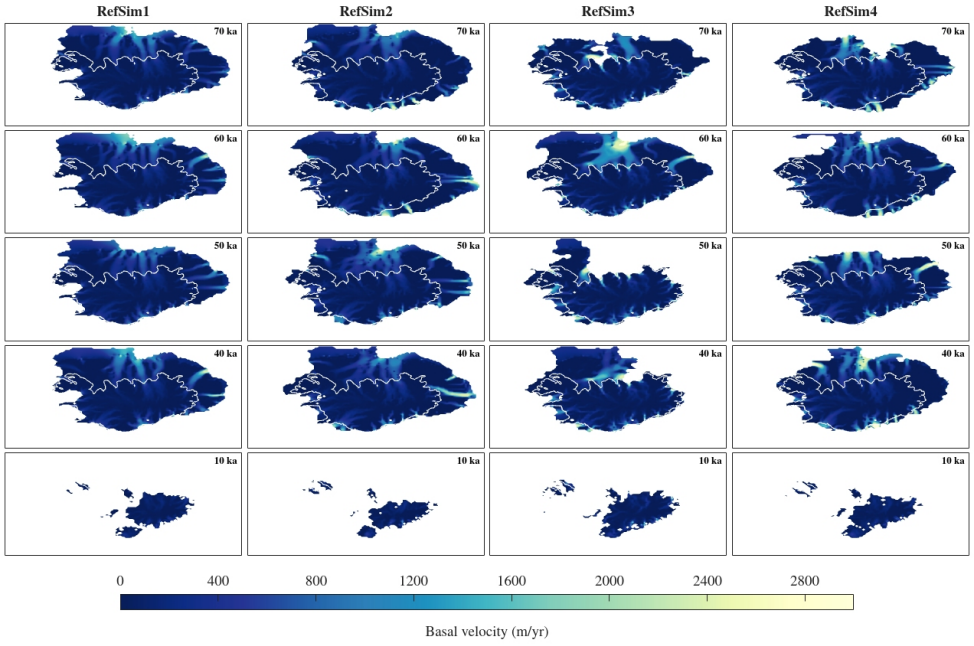

Figure S7. Basal velocity fields of the IIS for 4 $\text{NROY}_{\text{tier1}}$ runs (run identification number ic10593, ic10114, ic1184, and ic1468) at different times.

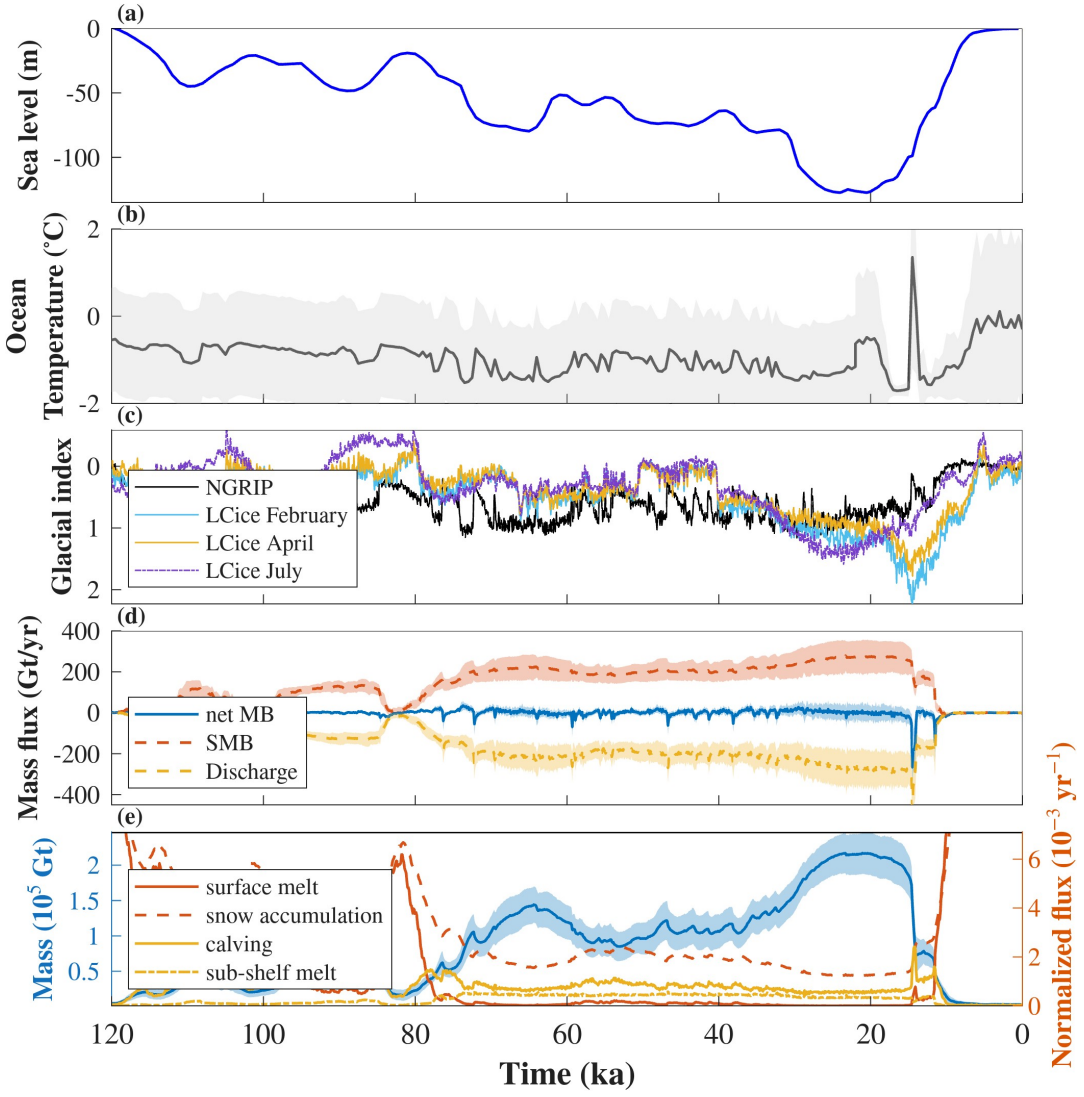

Figure S8. Climate forcing (input) and mass balance components (output) of the IIS over the last glacial cycle (120-0 ka) for the $\text{NROY}_{\text{tier1}}$ subset. (a) Global mean eustatic sea level reconstruction. (b) Ocean temperature at 191 m depth from TraCE-21ka deglacial simulation (Liu et al., 2009), with the gray shading indicating uncertainty ($\pm 1\sigma$) around the mean (gray line). (c) Glacial indices derived from smoothed temperature anomalies (50 years running mean, interpolated to 50 year time steps) from the NGRIP ice core (North Greenland Ice Core Project members, 2004) and seasonal variations from the LCice model (February, April, and July, Geng et al., 2025). (d) Mass balance components of grounded ice including net mass balance (blue), surface mass balance (SMB, orange dashed), and ice discharge at the grounding line (yellow dashed), with shading indicating uncertainty ($\pm 1\sigma$). (e) Total ice mass (blue, left axis) and normalized mass fluxes (right axis) including surface melt, snow accumulation, calving, and sub-shelf melt.

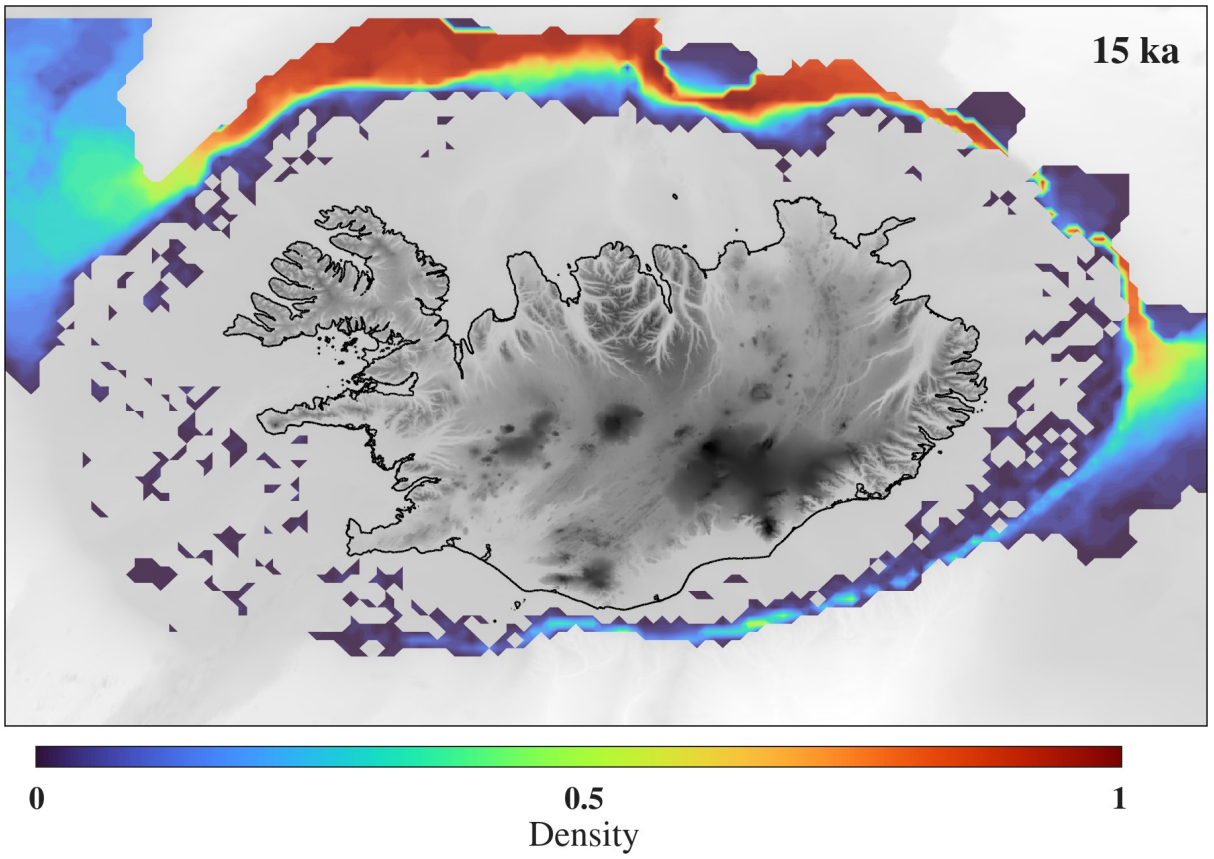

Figure S9. Density distribution of floating ice within the $\text{NROY}_{\text{tier1}}$ sub-ensemble at 15 ka. To avoid ice extending to the grid boundary, the GSM is configured to strongly calve ice where present-day depth is greater than 860 m, as indicated by the black dotted line.

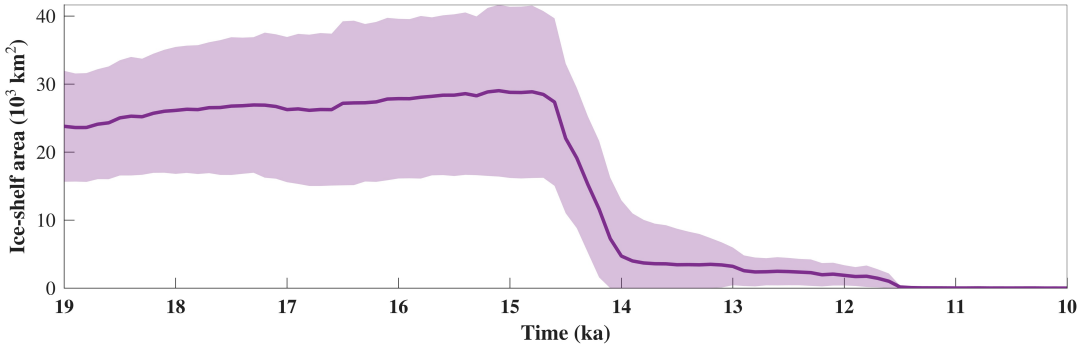

Figure S10. Time series of the ice shelf area during the last deglaciation for the $\text{NROY}_{\text{tier1}}$ subset. The line represents the means and the shaded area the 2σ range.

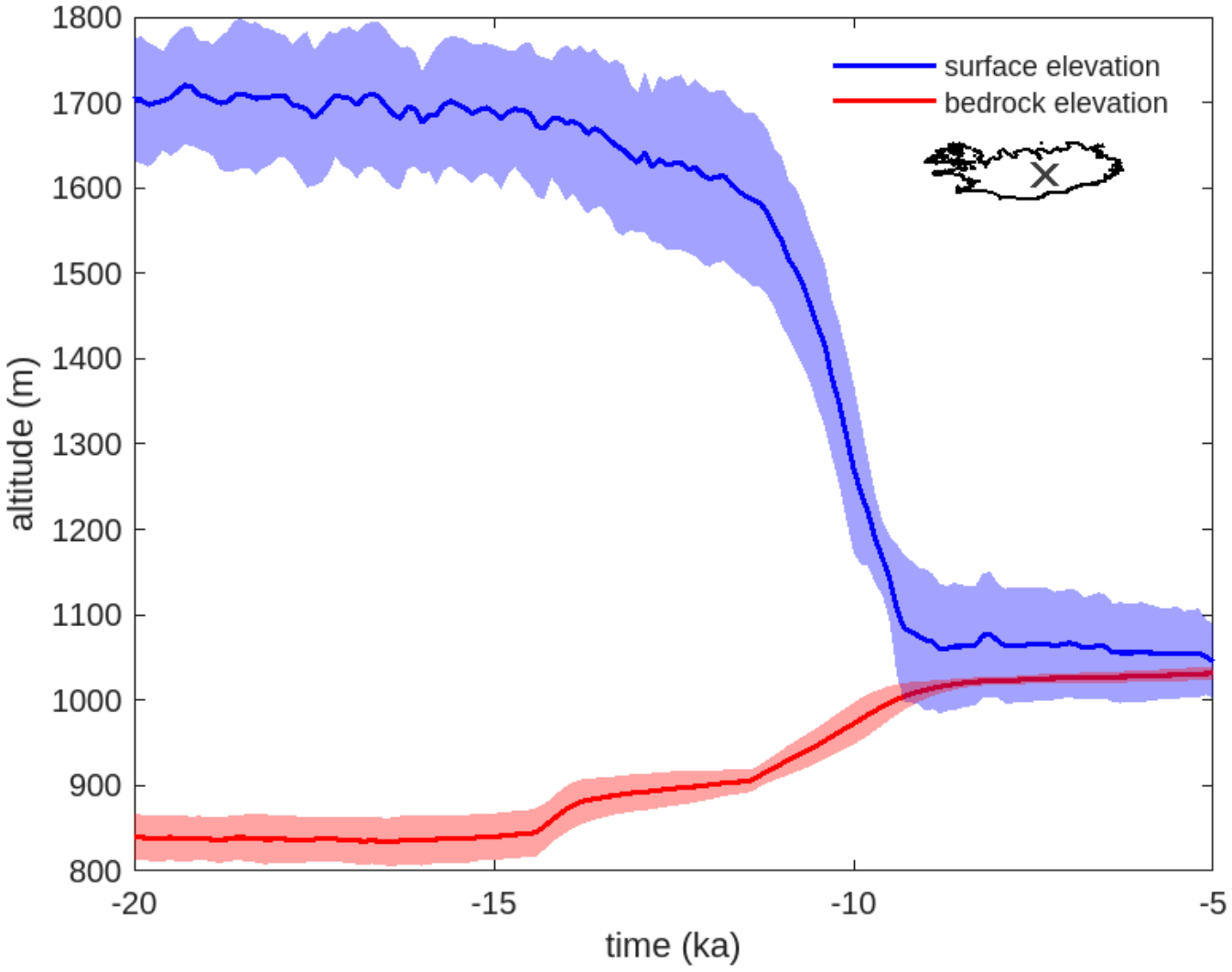

Figure S11. Surface and bedrock elevation at the center of the IIS for the $\text{NROY}_{\text{tier1}}$ subset. The lines represent the means and the shaded areas the 2σ range.

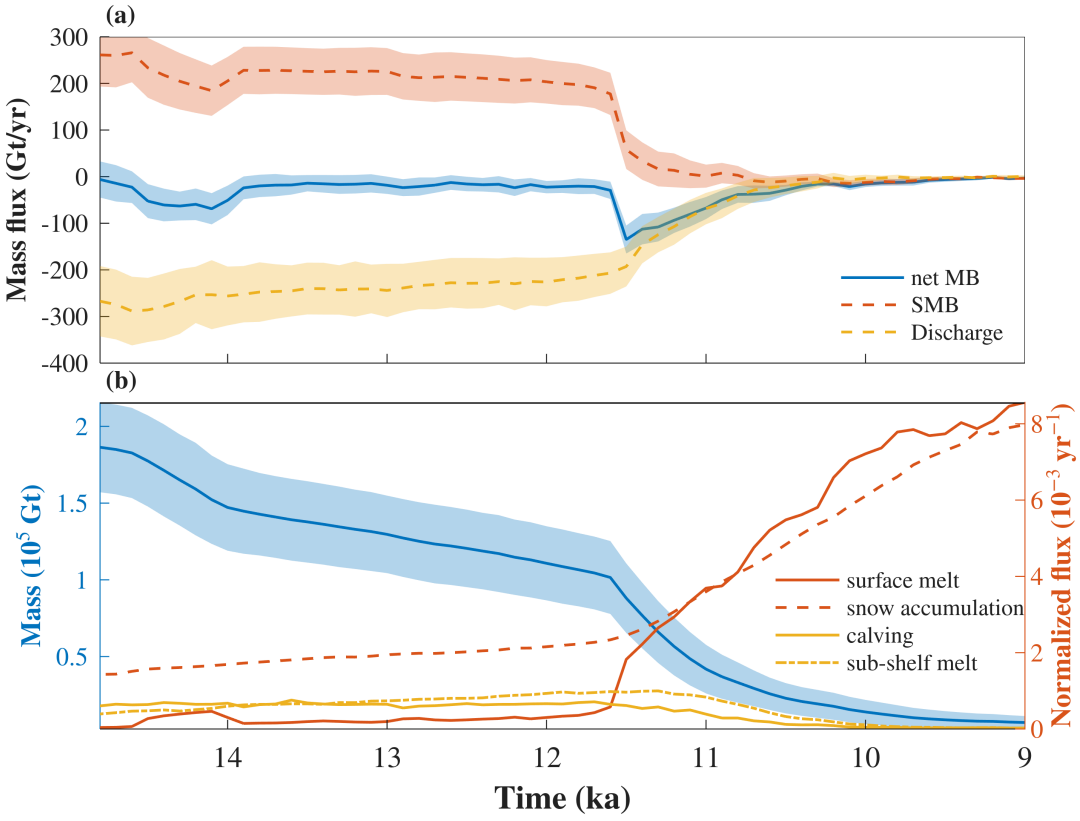

Figure S12. Mass balance components (output) of the IIS from 15 to 9 ka for experiments without hydrofracturing. (a) Mass balance components of grounded ice including net mass balance (blue), surface mass balance (SMB, orange dashed), and ice discharge at the grounding line (yellow dashed), with shading indicating uncertainty ($\pm 1\sigma$). (b) Total ice mass (blue, left axis) and mass fluxes normalized by the ice sheet total mass (right axis).

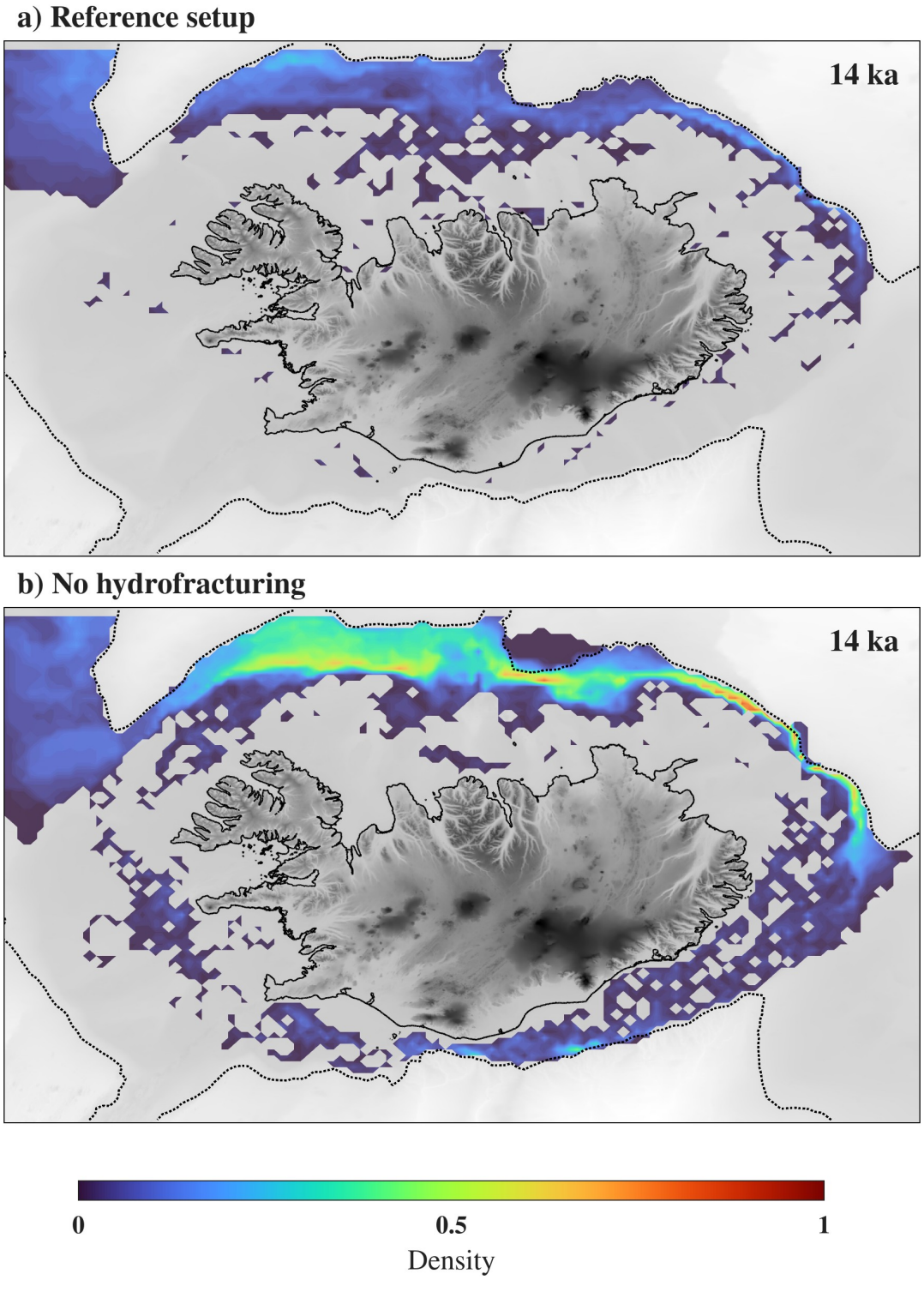

Figure S13. Density distribution of floating ice for the $NROY_{tier1}$ sub-ensemble (a) and for experiments without hydrofracturing (b) at 14 ka. The -860 m contour is represented by the black dotted line.

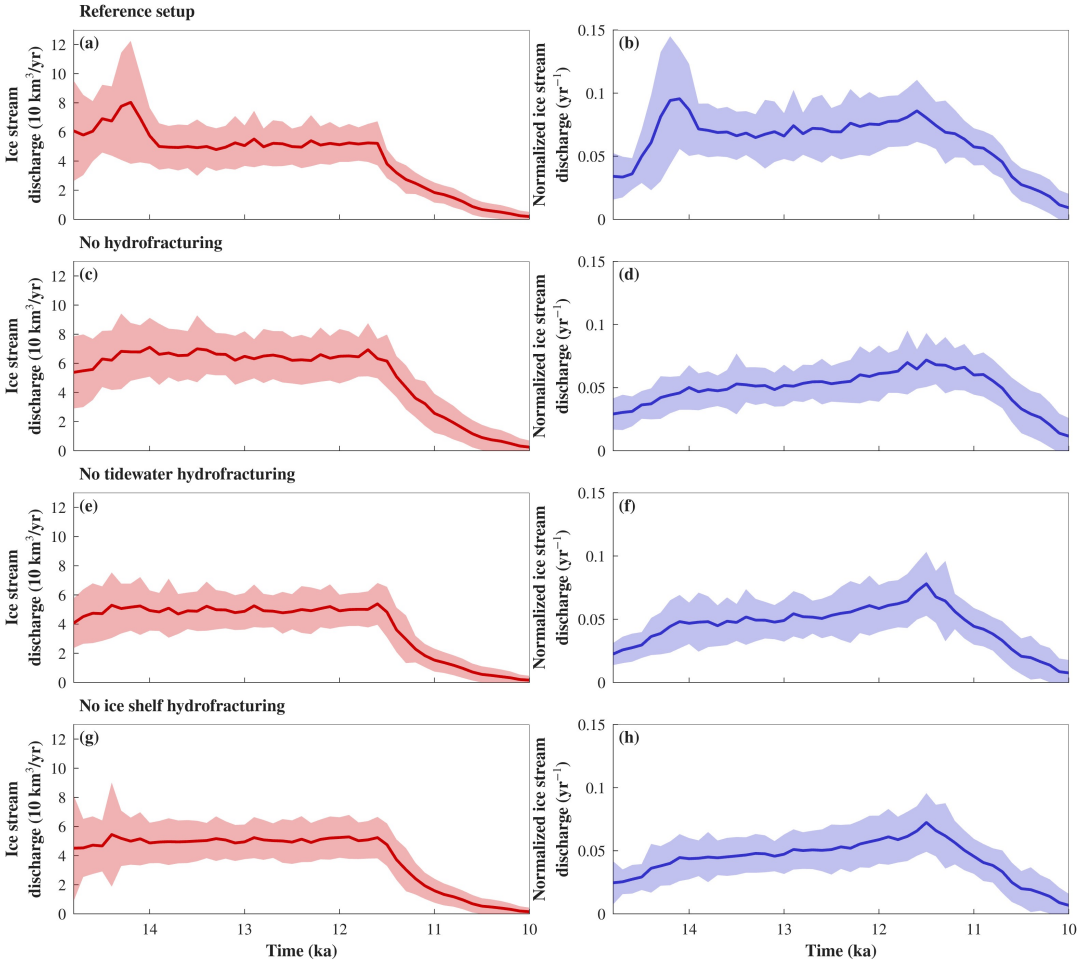

Figure S14. Ice stream discharge (left column) and ice stream discharge normalized by the ice sheet volume (right column) for the different tested sub-ensembles. The rows correspond to the $NROY_{tier1}$ reference setup (a, b), no hydrofracturing (c, d), no tidewater hydrofracturing (e, f), and no ice shelf hydrofracturing (g, h). The lines represent the means and the shaded areas the 2σ range. Ice stream discharge was calculated over gates placed within bathymetric troughs and valleys.

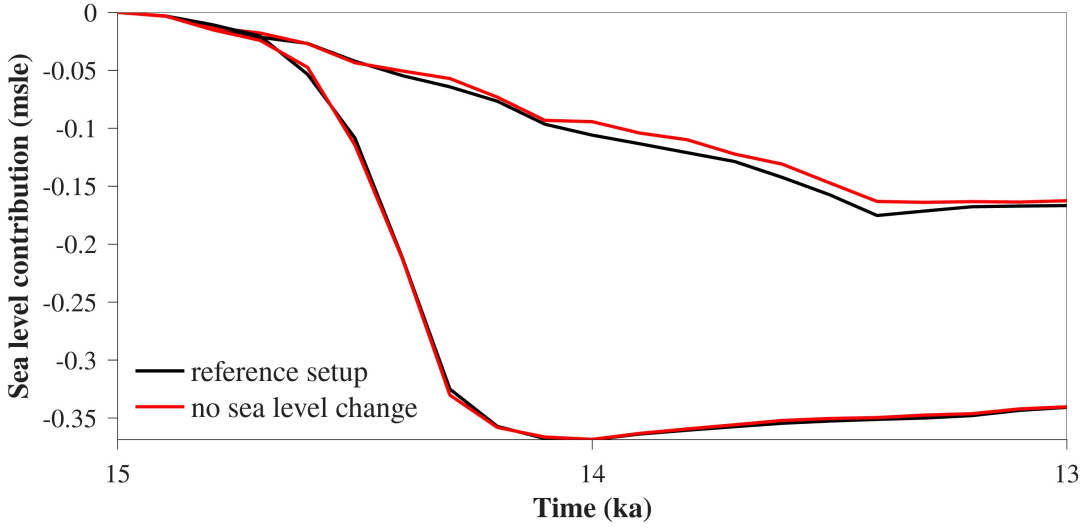

Figure S15. Sea level contribution relative to 15 ka from experiments with sea level change (black) and without sea level change (red) for 2 $NROY_{tier1}$ parameter vectors (run identification number ic1131, and ic1395, the latter showing the strongest sensitivity in the ensemble).

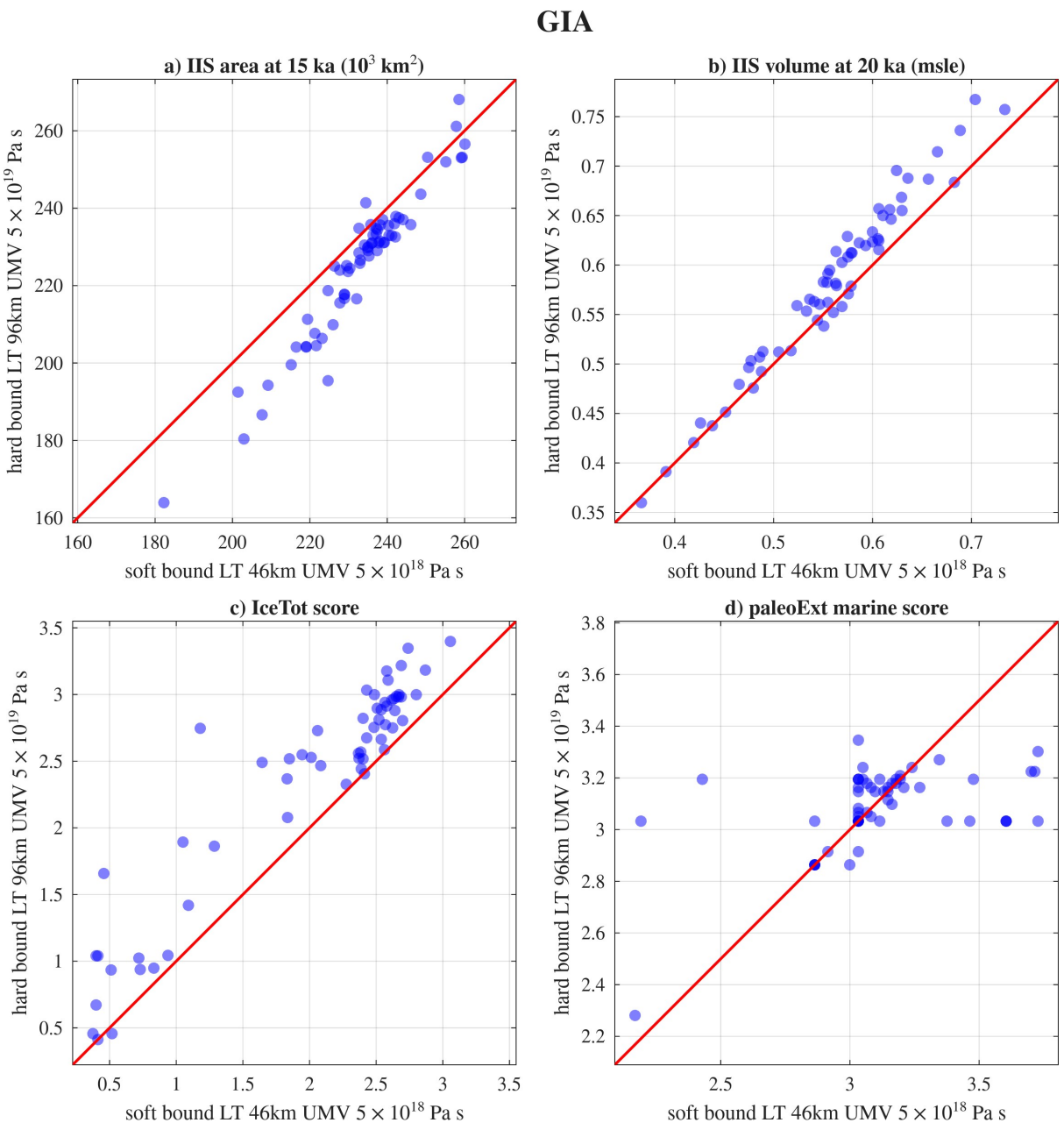

Figure S16. Sensitivity of the IIS to Glacial Isostatic Adjustment (GIA) Earth model parameters. Scatter plots compare a soft bound Earth model (lithosphere thickness 46 km, upper mantle viscosity 5×10^{18} Pa s; x-axis) against a hard bound Earth model (lithosphere thickness 96 km, upper mantle viscosity 5×10^{19} Pa s; y-axis). (a) IIS grounded ice area at 15 ka (10^3 km^2). (b) IIS ice volume at 20 ka (msle). (c) Total ice thickness misfit score (IceTot). (d) Marine paleo-extent misfit score (paleoExt). The red solid line indicates the 1:1 relationship.

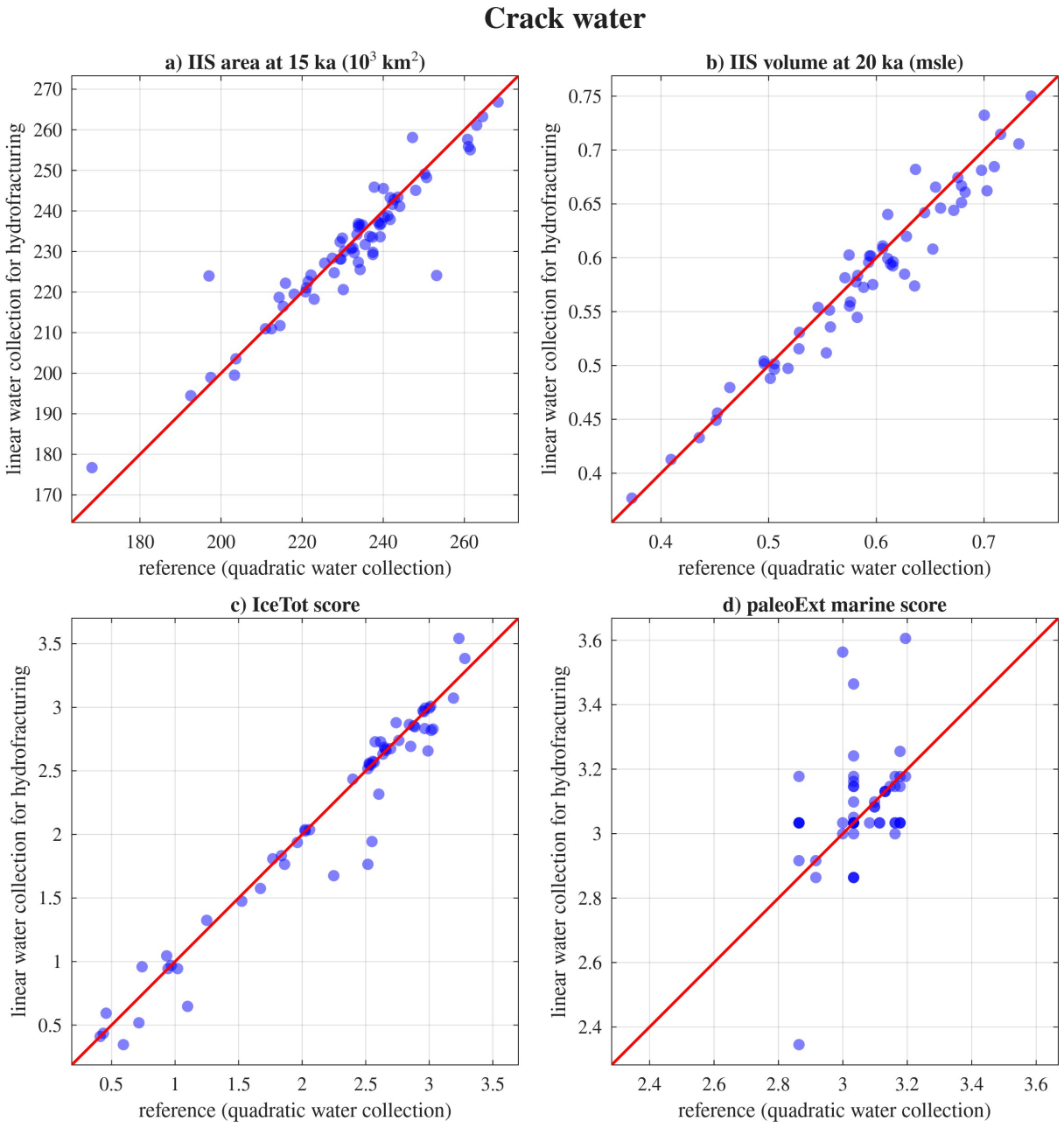

Figure S17. Sensitivity of the IIS to crack water collection parameterizations for hydrofracturing. Scatter plots compare the reference quadratic water collection (x-axis) against a linear water collection (y-axis). (a) IIS grounded ice area at 15 ka (10^3 km^2). (b) IIS ice volume at 20 ka (msle). (c) Total ice thickness misfit score (IceTot). (d) Marine paleo-extent misfit score (paleoExt). The red solid line indicates the 1:1 relationship.

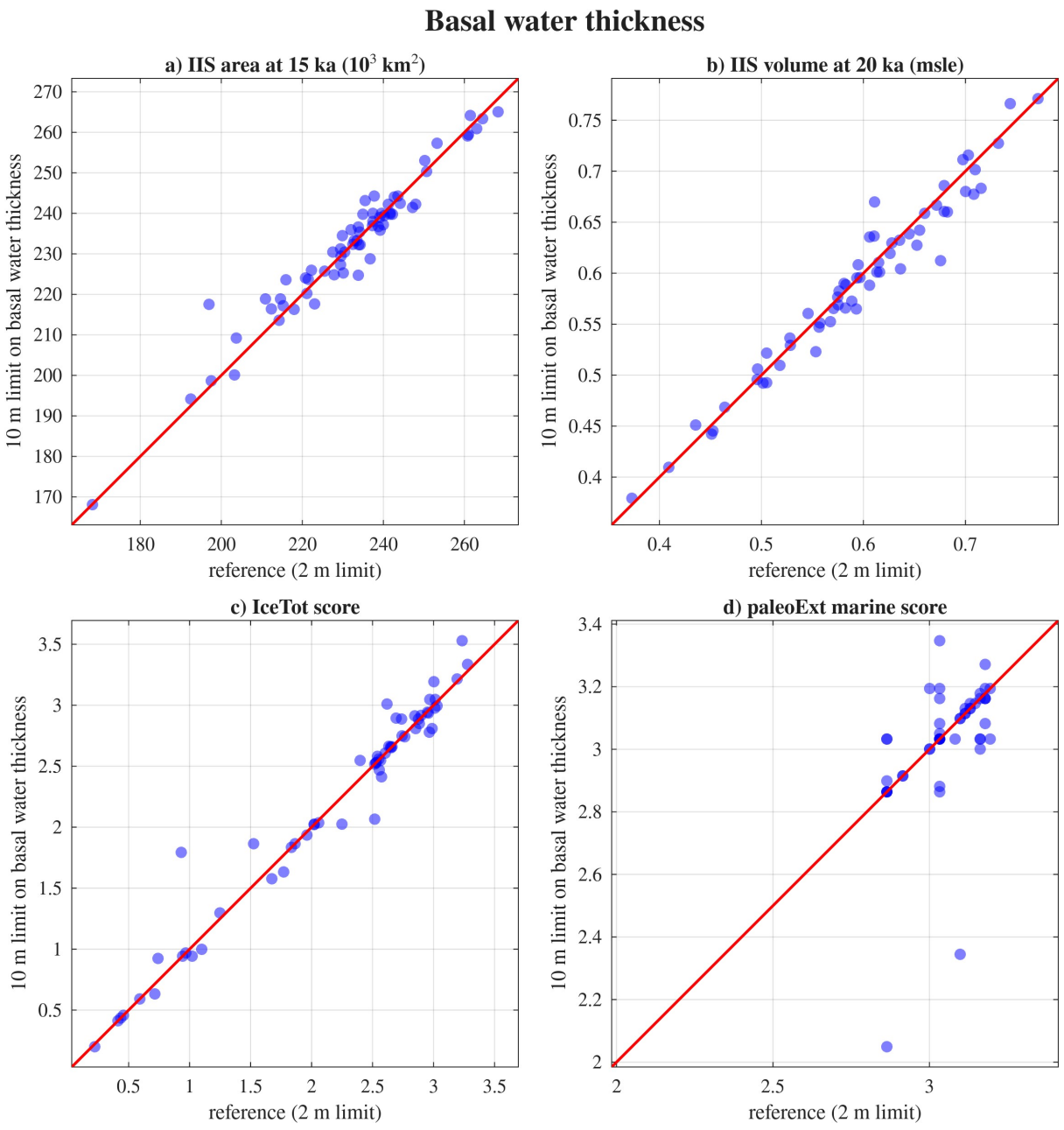

Figure S18. Sensitivity of the IIS to the basal water thickness limit. Scatter plots compare the reference 2 m limit (x-axis) against a 10 m limit on basal water thickness (y-axis). (a) IIS grounded ice area at 15 ka (10^3 km^2). (b) IIS ice volume at 20 ka (msle). (c) Total ice thickness misfit score (IceTot). (d) Marine paleo-extent misfit score (paleoExt). The red solid line indicates the 1:1 relationship.

References

Flóvenz, Ó. G. and Saemundsson, K.: Heat flow and geothermal processes in Iceland, Tectonophysics, 225, 123–138, https://doi.org/10.1016/0040-1951(93)90253-G, 1993.

Geng, M. S., Tarasov, L., and Dalton, A. S.: A comparison of the last two glacial inceptions (MIS 7/5) via fully coupled transient ice and climate modeling, EGUsphere, 2025, 1–47, https://doi.org/10.5194/egusphere-2025-495, 2025.

Hjartarson, Á.: Heat Flow in Iceland, World Geothermal Congress 2015, pp. 1–4, 2015.

Liu, Z., Otto-Bliesner, B. L., He, F., Brady, E. C., Tomas, R., Clark, P. U., Carlson, A. E., Lynch-Stieglitz, J., Curry, W., Brook, E., Erickson, D., Jacob, R., Kutzbach, J., and Cheng, J.: Transient simulation of last deglaciation with a new mechanism for bolling-allerod warming, Science, 325, 310–314, https://doi.org/10.1126/science.1171041, 2009.

North Greenland Ice Core Project members: High-resolution record of Northern Hemisphere climate extending into the last interglacial period, Nature, 431, 147–151, 2004.